


Robust Nuclear Spin Entanglement via Dipolar Interactions in Polar Molecules

Timur V. Tscherbul¹, Jun Ye², and Ana Maria Rey²

¹*Department of Physics, University of Nevada, Reno, Nevada 89557, USA*

²*JILA, National Institute of Standards and Technology, and Department of Physics, University of Colorado, Boulder, Colorado 80309, USA*

 (Received 30 April 2022; accepted 13 March 2023; published 6 April 2023)

We propose a general protocol for on-demand generation of robust entangled states of nuclear and/or electron spins of ultracold $^1\Sigma$ and $^2\Sigma$ polar molecules using electric dipolar interactions. By encoding a spin-1/2 degree of freedom in a combined set of spin and rotational molecular levels, we theoretically demonstrate the emergence of effective spin-spin interactions of the Ising and XXZ forms, enabled by efficient magnetic control over electric dipolar interactions. We show how to use these interactions to create long-lived cluster and squeezed spin states.

DOI: [10.1103/PhysRevLett.130.143002](https://doi.org/10.1103/PhysRevLett.130.143002)

Ultracold polar molecules hold great promise for quantum simulation, metrology, and information processing because they feature strong electric dipolar (ED) interactions that are both long range, anisotropic, and, more importantly, tunable [1–16]. A necessary condition toward their use for these goals is the capability to take advantage of their intrinsic ED interactions to create highly entangled and long-lived molecular states that are robust to environmental decoherence, such as spin-squeezed states for enhanced sensing [17–19], or cluster states for measurement-based quantum computation [20–25].

Up to date, rotational states of simple alkali molecules such as KRb have been proposed as the primary workhorse and a natural degree of freedom to encode a qubit [1–12]. This is because the long-lived rotational states can be directly coupled by long-range ED interactions and manipulated by microwave (mw) fields [26,27]. Nevertheless, rotational states feature important limitations that have hindered their use for entanglement generation: (1) ultracold molecules prepared in different rotational states typically experience different trapping potentials and therefore are subject to undesirable decoherence, leading to short coherence times [28–30]; (2) fine tuning of the many-body Hamiltonian parameters requires the use of strong and well-controlled dc electric fields E [1,11]. As these fields take time to switch and change, on-demand generation of entanglement using long-range ED interactions between rotational states remains a significant experimental challenge.

To overcome these important limitations, here we propose to leverage a larger set of internal levels accessible in ultracold polar molecules, which include nuclear and/or electron spin levels in addition to their rotational structure. Taken together, these levels can be used as a robust resource for on-demand entanglement generation. By encoding an effective spin-1/2 into a combined set of nuclear spin and rotational molecular levels, we take advantage of the long

coherence times enjoyed by nuclear spin levels and the strong ED interactions experienced by rotational levels at different stages of the entanglement generation process. We note that other types of qubit encodings have been suggested in Refs. [4,5]. Our proposal, in addition to the electric tunability of dipole-induced spin-exchange and Ising couplings, offers magnetic tunability of the ED interactions, and the ability to turn off exchange interactions on demand even at finite E fields. The magnetic tunability, an essential advantage of our approach, arises from inducing avoided crossings of electron spin-rotational levels of the opposite parity in $^2\Sigma$ molecules such as YO [31–34], CaF [35,36], and SrF [37,38], which have already been cooled down and trapped in optical potentials. We also show how to engineer magnetically tunable level crossings in $^1\Sigma$ molecules via mw dressing. In this way, we can engineer spin models of Ising and XXZ types with an enlarged set of control parameters.

Entangling nuclear spins of $^1\Sigma$ molecules: Ising interactions and cluster states.—Consider an ensemble of ultracold $^1\Sigma$ molecules confined to a single plane of a three-dimensional (3D) optical lattice at unit filling as shown in Fig. 1(a). To entangle the nuclear spins of the molecules via ED interactions, we propose to encode an effective spin-1/2 into the states $|\uparrow\rangle = |\tilde{0}0, M\rangle$ and $|\downarrow\rangle = |\tilde{1}0, M'\rangle$ as shown in Fig. 2(a). We refer to these states as nuclear spin-rotational states. Here, $|\tilde{N}M_N, M\rangle$ denote molecular eigenstates in the limit of large magnetic field B , where the nuclear spin projections on the field axis $M = \{M_{I_1}, M_{I_2}\}$ are good quantum numbers [26,39]. At zero E field the rotational quantum number N is a good quantum number with the rotational energy spacing set by the rotational constant B_e . At finite E field, the rotational states admix but we can still label the states that adiabatically connect to zero-field N -states as \tilde{N} [40]. We further assume that the external E and B fields are parallel.

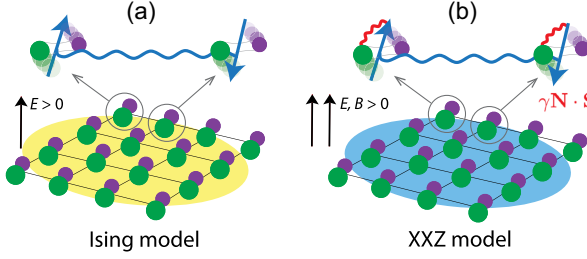


FIG. 1. (a) Experimental setup for nuclear spin entanglement generation consisting of $^1\Sigma$ molecules in superpositions of spin-rotational states trapped in an optical lattice on a 2D plane. Molecular spins (arrows) interact via the long-range Ising interaction (wavy line), creating cluster-state entanglement represented by the yellow shaded area. (b) Same as (a) but in the presence of a B field and the spin-rotation interaction (red wavy lines) near an avoided crossing in $^2\Sigma$ molecules. The blue shaded area represents entanglement of the XXZ type leading to the generation of spin-squeezed states.

Importantly, we require that our effective spin-1/2 states have *different* nuclear spin projections ($M \neq M'$), which ensures that the off-diagonal matrix elements of the molecular electric dipole moment (EDM) \hat{d} are strongly suppressed ($\langle \uparrow | \hat{d} | \downarrow \rangle = d_{\uparrow\downarrow} \rightarrow 0$). This is because in the large B -field limit, the electric quadrupole interaction, becomes small compared to the Zeeman interaction [41], and M and M_N become good quantum numbers. This property makes our encoding distinct from the one proposed in all of the previous theoretical work, which used rotational states with $M = M'$ [1–4,6–8,11]. The only exception is Ref. [64], which proposed the use of a combination of electron spin and rotational states near avoided level crossings to engineer interqubit interactions using infrared laser pulses. In our work, these interactions arise naturally without the need to use extra pulses or avoided crossings (except in the specific case of the XXZ model with $^1\Sigma$ molecules as discussed below).

In the absence of an external E field, all matrix elements of the EDM vanish identically in our effective spin-1/2 basis [see Fig. 2(a)], as the basis states have a definite parity. As a result, the long-range ED interaction between the molecules also vanishes. When an E field is applied, the diagonal matrix elements $d_{\uparrow} = \langle \uparrow | \hat{d} | \uparrow \rangle$ and $d_{\downarrow} = \langle \downarrow | \hat{d} | \downarrow \rangle$ acquire finite values with $d_{\uparrow} \neq d_{\downarrow}$, as shown in Fig. 2(b), whereas $d_{\uparrow\downarrow} \rightarrow 0$ (see above). This leads to the emergence of ED interactions between molecules in the different nuclear spin-rotational states described by the long-range Ising model [41]

$$\hat{H}_{\text{dip}} = \sum_{i>j} J_{ij}^z \hat{S}_i^z \hat{S}_j^z, \quad (1)$$

where the effective spin-1/2 operators \hat{S}_i^z act in the two-dimensional Hilbert space of the i th molecule $\{|\downarrow\rangle, |\uparrow\rangle\}$,

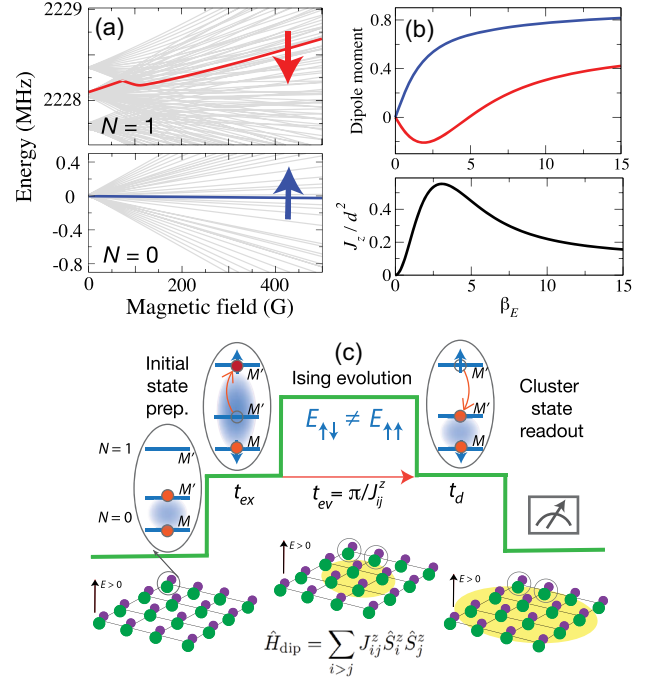


FIG. 2. (a) Zeeman energy levels of a typical bialkali molecule (here, $^{40}\text{K}^{87}\text{Rb}$). Our effective spin-1/2 states $|\uparrow\rangle = |\tilde{0}0, M\rangle$ and $|\downarrow\rangle = |\tilde{1}0, M'\rangle$ are marked by arrows. (b) Expectation values of the EDM d_{\uparrow} (top curve) and d_{\downarrow} (bottom curve) and the Ising coupling constant J_z (bottom panel) as a function of the reduced E -field strength $\beta_E = dE/B_e$ [40]. (c) Protocol for creating long-lived nuclear spin cluster states of polar molecules via ED interactions.

$J_{ij}^z = (d_{\uparrow} - d_{\downarrow})^2 (1 - 3\cos^2\theta_{ij}) / |\mathbf{R}_{ij}|^3$ is the Ising coupling constant, \mathbf{R}_{ij} is the distance vector between the molecular centers of mass, and θ_{ij} is the angle between \mathbf{R}_{ij} and the direction of the E field. The E -field dependence of J_{ij}^z shown in Fig. 2(b) reaches a maximum at $\beta_E = Ed/B_e \simeq 3$.

Importantly, because our effective spin-1/2 states correspond to the $\tilde{N} = 0$ and $\tilde{N} = 1$ Stark levels, the Ising interaction between the molecules in different nuclear spin-rotational states ($M \neq M'$) is as strong as that between the molecules in ordinary rotational states ($M = M'$) [10].

The starting point of our general entanglement-generating protocol is an ensemble of $\tilde{N} = 0$ molecules trapped in a single plane of a 3D optical lattice as shown in Fig. 2(c). The molecules are initialized in a coherent superposition of two different $\tilde{N} = 0$ nuclear spin states $|\tilde{0}0, +\rangle = (1/\sqrt{2})[|\tilde{0}0, M\rangle + |\tilde{0}0, M'\rangle]$. No long-range interactions are initially present between the molecules, since $d_{\uparrow} = d_{\downarrow}$ for all $\tilde{N} = 0$ nuclear spin states even in the presence of a dc E field, and thus $J_{ij}^z = 0$. As an example, we consider ultracold $\text{KRb}(^1\Sigma^+)$ molecules prepared in a coherent superposition of two nuclear spin states $|\tilde{0}0, +\rangle_{\text{KRb}} = (1/\sqrt{2})[|\tilde{0}0, -3, -1/2\rangle + |\tilde{0}0, -4, 1/2\rangle]$, which can be realized experimentally via two-photon

microwave excitation [26,65]. Further analysis of the experimental feasibility of our protocol [41] shows that most of the requisite experimental tools have already been implemented in the laboratory, and thus its experimental realization appears feasible with current or near-future technology.

In Step 1, we initialize our spin-rotational qubits by preparing a coherent superposition $|+\rangle = (1/\sqrt{2})(|\uparrow\rangle + |\downarrow\rangle)$ [see Fig. 2(c)]. This can be achieved by starting with the coherent superposition of $\tilde{N} = 0$ nuclear spin states $|\tilde{0}0, +\rangle$ defined above, and applying a resonant pulse of mw radiation on the $|\tilde{0}0, M'\rangle \rightarrow |\tilde{1}0, M'\rangle$ rotational transition.

Figure 3(a) illustrates the idea for KRb. By applying a mw π pulse to the superposition $|\tilde{0}0, +\rangle_{\text{KRb}}$ resonant on the $|\tilde{0}0, -4, 1/2\rangle \rightarrow |\tilde{1}0, -4, 1/2\rangle$ transition (which has a large transition dipole moment), the population in the $|\tilde{0}0, -4, 1/2\rangle$ state is coherently transferred to the rotationally excited state, leading to the desired superposition $|+\rangle_{\text{KRb}} = (1/\sqrt{2})(|\tilde{0}0, -3, -1/2\rangle + |\tilde{1}0, -4, 1/2\rangle)$. To show that it is possible to selectively excite a single eigenstate component of the initial superposition, (i.e., $|\tilde{0}0, -4, 1/2\rangle$ but not $|\tilde{0}0, -3, -1/2\rangle$), we plot in Fig. 3(b) the energy difference between the main transition ($|\tilde{0}0, -4, 1/2\rangle \leftrightarrow |\tilde{1}0, -4, 1/2\rangle$) and the competing transition. The differential Stark shift is seen to be negative at small E fields, approaching zero at $E \simeq 10$ kV/cm. Thus, selective mw excitation of the desired transition $|\tilde{0}0, -4, 1/2\rangle \rightarrow |\tilde{1}0, -4, 1/2\rangle$ is possible by tuning the E field below 5 kV/cm or above 15 kV/cm, where the competing transition is energetically detuned.

In Step 2, we let our initial n -molecule superposition $|+\rangle^{\otimes n}$ evolve under the Ising interaction for the cluster time $t_c = \pi/|J_{i,i+1}^z|$. Because of the long-range nature of the interaction, the resulting proxy cluster state will be different

from the proper cluster state formed under nearest-neighbor (NN) interactions [20,21]. Nevertheless, theoretical simulations in 1D show that cluster-state fidelities above 75% can be achieved for ≤ 12 molecules even in the presence of moderately strong ($|J_{i,i+2}^z/J_{i,i+1}^z| = 0.1$) next-NN interactions [66]. These interactions can also be efficiently suppressed using dynamical decoupling techniques [66].

At $t = t_c$ a maximally entangled cluster state of nuclear spin-rotational qubits is created [20,24]. The Ising coupling constant $J_{i,i+1}^z$ is plotted for the NN interactions of KRb molecules in Fig. 3(c). At $E = 20$ kV/cm and the NN spacing of 500 nm, $J_{i,i+1}^z/2\pi = 30$ Hz and it takes $t_c \simeq 16.7$ ms to evolve the lattice-confined ensemble of KRb molecules into the highly entangled cluster state. Preserving the coherence during Ising evolution is experimentally feasible because the coherence times T_2 of the nuclear spin-rotational superpositions are likely to be similar to those of purely rotational superpositions [65,67], with $T_2 = 470$ ms demonstrated for CaF [30]. A detailed analysis of the effects of decoherence on cluster states is presented in the Supplemental Material [41].

In Step 3, we coherently transfer population back to the ground rotational state via the $|\tilde{1}0, M'\rangle \rightarrow |\tilde{0}0, M'\rangle$ transition. After the de-excitation step, the molecules find themselves once again in a coherent superposition of $\tilde{N} = 0$ nuclear spin sublevels $|\tilde{0}0, +\rangle = (1/\sqrt{2})(|\tilde{0}0, M\rangle + |\tilde{0}0, M'\rangle)$. The long-range Ising interaction is thereby completely turned off, preserving the entanglement created in Step 2. We expect the resultant nuclear spin cluster state to be both long-lived and robust due to the much longer coherence times of $\tilde{N} = 0$ nuclear spin qubits compared to their rotational counterparts [65,67]. These advantages of our protocol enable long-term storage of quantum information in the cluster state encoded in molecular nuclear spins, enabling efficient implementation of the measurement protocols of one-way quantum computing [21,22].

We next consider the question of how to engineer a more general XXZ-type interaction between the electron spins of $^2\Sigma$ molecules or nuclear spins of $^1\Sigma$ molecules. While this interaction arises naturally between the different rotational states with $M = M'$ [11,40], it requires finite off-diagonal EDM matrix elements, which are absent in the basis of nuclear spin-rotation states we have considered so far. Thus, in order to obtain a nonzero spin exchange coupling, it is necessary to break the spin symmetry. Here, we consider two symmetry-breaking scenarios that rely on the spin-rotation interaction in $^2\Sigma$ molecules and on mw-dressed rotational states of $^1\Sigma$ molecules.

As a specific example, consider the YO($^2\Sigma$) molecule recently laser cooled [33] and trapped in an optical lattice [34]; see Fig. 4(e). A remarkable feature of YO is its extremely large hyperfine interaction, which dominates over the spin-rotation interaction and results in the total spin angular momentum $\mathbf{G} = \mathbf{I} + \mathbf{S}$ being a good

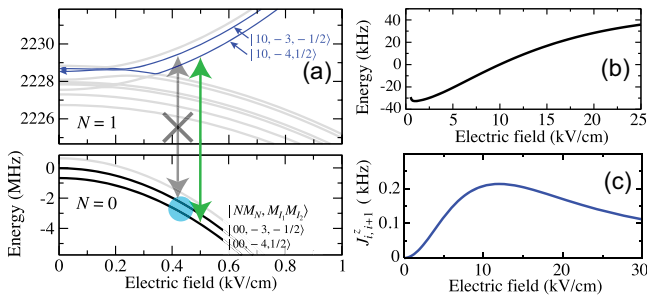


FIG. 3. (a) Energy levels of $^{40}\text{K}^{87}\text{Rb}$ used in our entanglement generation protocol plotted vs E field at $B = 400$ G and $M_F = M_N + M_{I_K} + M_{I_{Rb}} = -7/2$. The initial coherent superposition of the $\tilde{N} = 0$ nuclear spin states is marked with a blue circle. The mw transition used to excite the initial coherent superposition $|+\rangle$ is marked with a green arrow. The competing mw transition is marked by the gray arrow. The differential Stark shift (b) and the NN Ising constant (c) plotted vs E field for $^{40}\text{K}^{87}\text{Rb}$ molecules at the lattice spacing of 500 nm.

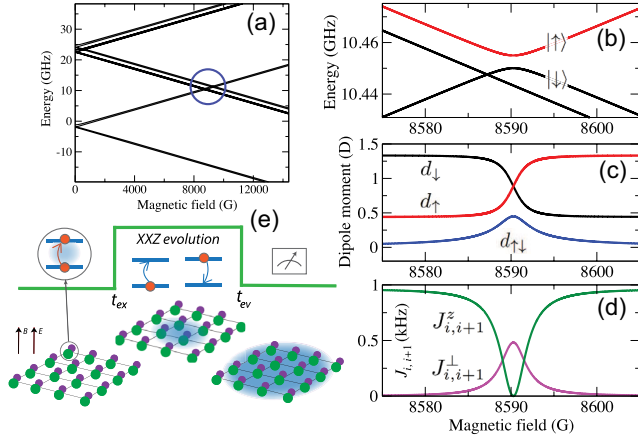


FIG. 4. (a) Zeeman energy levels of YO at $E = 5$ kV/cm. The ALC between the levels $|\tilde{0}0, 1/2 M_I\rangle$ and $|\tilde{1}1, -1/2 M_I\rangle$ is marked with a circle. Energy levels (b), EDM matrix elements (c), and NN spin coupling constants $J_{i,i+1}^z$ and $J_{i,i+1}^\perp$ (d) plotted as a function of B field near the ALC at the NN spacing of 500 nm. (e) Experimental protocol for creating long-lived spin-squeezed states of YO molecules.

quantum number [32] at low B fields, where \mathbf{I} and \mathbf{S} are the nuclear and electron spins, respectively. In the large B -field limit, the spin-rotational states of $\text{YO}(^2\Sigma)$ $|\tilde{N}M_N, M_S M_I\rangle$, have well-defined values of nuclear (M_I) and electron (M_S) spin projections on the field axis.

Figure 4(a) shows the lowest rotational energy levels of $\text{YO}(^2\Sigma)$. The opposite-parity levels $|\tilde{0}0, 1/2 M_I\rangle$ and $|\tilde{1}1, -1/2 M_I\rangle$ cross at $B_c \simeq 0.85$ T [68–70]. At $B = B_c$ and $E > 0$, the electron spin-rotation interaction mixes the levels, leading to an avoided level crossing (ALC) shown in Fig. 4(b), and we choose our effective spin-1/2 states $|\alpha\rangle = |\uparrow\rangle, |\downarrow\rangle$ as

$$|\alpha\rangle = c_{a1}|\tilde{0}0, \frac{1}{2} M_I\rangle + c_{a2}|\tilde{1}1, -\frac{1}{2} M_I\rangle, \quad (2)$$

where c_{ai} are B -dependent mixing amplitudes [41]. Thus, in the vicinity of the ALC, the electron spin and rotation mixing provides $d_{\uparrow\downarrow} \neq 0$, which gives rise to the XXZ interaction [41]

$$\hat{H}_{\text{dip}}^{\text{ex}} = \sum_{i>j} \left[\frac{1}{2} J_{ij}^\perp (\hat{S}_i^+ \hat{S}_j^- + \text{H.c.}) + J_{ij}^z \hat{S}_i^z \hat{S}_j^z \right], \quad (3)$$

where $J_{ij}^\perp = 2d_{\uparrow\downarrow}^2 (1 - 3\cos^2\theta_{ij})/|\mathbf{R}_{ij}|^3$ is the spin-exchange coupling constant. As shown in Figs. 4(c) and 4(d), because the spin mixing in Eq. (2) is localized in the vicinity of the ALC, both $d_{\uparrow\downarrow}$ and J_{ij}^\perp peak at $B = B_c$, where $|c_{ai}| = 1/\sqrt{2}$. The diagonal matrix elements of the EDM become equal at $B = B_c$, where J_{ij}^z vanishes [see Fig. 4(d)]. The remarkable magnetic tunability of the spin coupling constants near ALCs can be used to vary the ratio J_{ij}^z/J_{ij}^\perp

over a wide range. Achieving such tuning of J_{ij}^z/J_{ij}^\perp is desirable for accessing new regimes of spin-squeezing dynamics depending on the sign of $J^z - J^\perp$ [71] and quantum simulation, since its tunability is far from straightforward in traditional protocols that rely on pure rotational states, requiring the use of multiple mw fields [11].

To realize the spin-squeezed states experimentally, we propose to use a standard Ramsey protocol shown in Fig. 4(e), in which mw fields are used to excite the initial coherent superposition $(1/\sqrt{2})[|\uparrow\rangle + |\downarrow\rangle]$ (as recently realized in a beam experiment [72]) and during the dark time the system is allowed to evolve under the XXZ Hamiltonian.

The evolution leads to the formation of a spin-squeezed state in the $\{|\uparrow\rangle, |\downarrow\rangle\}$ basis [19]. At the last step, the B field is adiabatically ramped down to transfer the $|\uparrow\rangle$ and $|\downarrow\rangle$ states back to the $|\tilde{0}0, 1/2 M_I\rangle$ and $|\tilde{1}1, -1/2 M_I\rangle$ zeroth-order states, and the latter state is coherently transferred to the $|\tilde{0}0, -1/2 M_I\rangle$ state using a circularly polarized mw π pulse. As a result, we obtain a long-lived squeezed state of electron spins of $\tilde{N} = 0$ $^2\Sigma$ molecules, which can be used to measure, e.g., external B fields. The effects of decoherence on spin-squeezed states can be efficiently mitigated [41] as long as the evolution time remains much smaller than the single-molecule coherence time, as is currently the case for, e.g., YO and CaF.

The above scenario of generating magnetically tunable XXZ interactions is clearly unfeasible for $^1\Sigma$ molecules due to their extremely small nuclear magnetic moments. To overcome this limitation, we use mw dressing to make the opposite-parity states degenerate as illustrated in Fig. 5(a). Specifically, driving the transition between the states

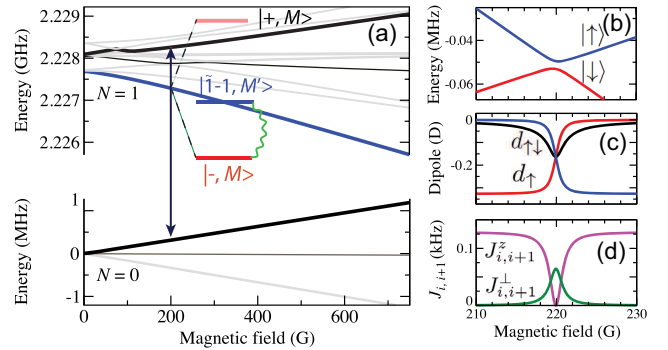


FIG. 5. (a) Mw-dressed states $|\pm, M\rangle$ (red bars) of $^{40}\text{K}^{87}\text{Rb}$ for $M_F = 7/2$ obtained by driving the mw transition (vertical arrow, $\Omega/2\pi = 2.1$ MHz) between the bare levels $|\tilde{0}0, -2, -3/2\rangle$ and $|\tilde{1}0, -2, -3/2\rangle$. The effective spin-1/2 is encoded into the mw-dressed state $|- , M\rangle$ and the bare state $|\tilde{1}-1, -4, 3/2\rangle$ (blue bar), which are coupled by the electric quadrupole interaction (wavy line). B -field dependence of the effective spin-1/2 energy levels (b), EDM matrix elements (c), and NN XXZ spin coupling constants $J_{i,i+1}^\perp$ and $J_{i,i+1}^z$ (d) near the ALC.

$|\tilde{0}0, M\rangle$ and $|\tilde{1}0, M\rangle$ (such as the $|\tilde{0}0, -2, -3/2\rangle$ and $|\tilde{1}0, -2, -3/2\rangle$ states of KRb) by a linearly polarized mw field creates a pair of mw-dressed states in the rotating frame [10]

$$|\pm, M\rangle = c_0^\pm(\Omega, \Delta)|\tilde{0}0, M\rangle + c_1^\pm(\Omega, \Delta)|\tilde{1}0, M\rangle, \quad (4)$$

where the mixing coefficients c_N^\pm depend on the Rabi frequency Ω and the detuning from resonance Δ . For simplicity, we will consider the case of resonant driving ($\Delta = 0$), where the energies of the mw-dressed states $E_\pm = E_{1,M} \pm \Omega/2$ (assuming $\hbar = 1$), and $E_{1,M}$ is the energy of the bare state $|\tilde{1}0, M\rangle$. We note that the coherence time of these states could be limited by the different trapping potentials experienced by the $|\tilde{0}0, M\rangle$ and $|\tilde{1}0, M\rangle$ bare states, as well as by the coherence properties of the dressing field. Fortunately, it may be possible to choose the mixing coefficients c_N^\pm in such a way as to achieve state-insensitive trapping conditions [11,73].

To encode the effective spin-1/2, we choose the lowest-energy mw-dressed state $|-, M\rangle$ defined above and the bare state $|\tilde{1}-1, M'\rangle = |\tilde{1}-1, -4, 3/2\rangle$ of KRb shown in Fig. 5(a). These states are coupled by the electric quadrupole interaction [41] via the matrix element $V_{MM'} = \langle -, M | \hat{H}_{eQ} | \tilde{1}-1, M' \rangle = 1.8$ kHz. Figure 5(b) shows the energies of our effective spin-1/2 states $|\uparrow, \downarrow\rangle = c_M^{(\uparrow\downarrow)} |-, M\rangle + c_{M'}^{(\uparrow\downarrow)} |\tilde{1}-1, M'\rangle$ as a function of B field. The NN spin coupling constants $J_{i,i+1}^\perp$ and $J_{i,i+1}^z$ shown in Fig. 5(d) reach their maximal and minimal values at $B = B_c$. We note that $J_{ij}^z(B_c) = 0$ since $d_\uparrow = d_\downarrow$ at the ALC, and thus the ratio $J_{i,i+1}^\perp/J_{i,i+1}^z$ can be magnetically tuned over a wide dynamic range.

In summary, we have shown how to engineer long-lived cluster and spin-squeezed states using the nuclear spins of $^1\Sigma$ molecules and the electron spins of $^2\Sigma$ molecules in their ground rotational states. The proposed schemes can be applied to a wide range of polar molecules recently cooled and trapped in many laboratories [26,29–38], opening up a general path to long-lived spin entanglement generation in ultracold molecular ensembles.

We thank Junru Li and Jeremy Young for careful reading and feedback on the manuscript. This work was supported by the NSF EPSCoR RII Track-4 Fellowship (Grant No. 1929190), the AFOSR MURI, the NSF JILA-PFC PHY-1734006, and by NIST.

[1] D. DeMille, Quantum Computation with Trapped Polar Molecules, *Phys. Rev. Lett.* **88** (2002).

[2] A. André, D. DeMille, J.M. Doyle, M.D. Lukin, S.E. Maxwell, P. Rabl, R.J. Schoelkopf, and P. Zoller, A coherent all-electrical interface between polar molecules

and mesoscopic superconducting resonators, *Nat. Phys.* **2**, 636 (2006).

- [3] S.F. Yelin, K. Kirby, and R. Côté, Schemes for robust quantum computation with polar molecules, *Phys. Rev. A* **74**, 050301(R) (2006).
- [4] Q. Wei, S. Kais, B. Friedrich, and D. Herschbach, Entanglement of polar symmetric top molecules as candidate qubits, *J. Chem. Phys.* **135**, 154102 (2011).
- [5] M. Karra, K. Sharma, B. Friedrich, S. Kais, and D. Herschbach, Prospects for quantum computing with an array of ultracold polar paramagnetic molecules, *J. Chem. Phys.* **144**, 094301 (2016).
- [6] K.-K. Ni, T. Rosenband, and D.D. Grimes, Dipolar exchange quantum logic gate with polar molecules, *Chem. Sci.* **9**, 6830 (2018).
- [7] P. Yu, L. W. Cheuk, I. Kozyryev, and J. M. Doyle, A scalable quantum computing platform using symmetric-top molecules, *New J. Phys.* **21**, 093049 (2019).
- [8] M. L. Wall and L. D. Carr, Emergent timescales in entangled quantum dynamics of ultracold molecules in optical lattices, *New J. Phys.* **11**, 055027 (2009).
- [9] L. D. Carr, D. DeMille, R. V. Krems, and J. Ye, Cold and ultracold molecules: Science, technology and applications, *New J. Phys.* **11**, 055049 (2009).
- [10] A. V. Gorshkov, S. R. Manmana, G. Chen, J. Ye, E. Demler, M. D. Lukin, and A. M. Rey, Tunable Superfluidity and Quantum Magnetism with Ultracold Polar Molecules, *Phys. Rev. Lett.* **107**, 115301 (2011).
- [11] A. V. Gorshkov, S. R. Manmana, G. Chen, E. Demler, M. D. Lukin, and A. M. Rey, Quantum magnetism with polar alkali-metal dimers, *Phys. Rev. A* **84**, 033619 (2011).
- [12] B. Yan, S. A. Moses, B. Gadway, J. P. Covey, K. R. A. Hazzard, A. M. Rey, D. S. Jin, and J. Ye, Observation of dipolar spin-exchange interactions with lattice-confined polar molecules, *Nature (London)* **501**, 521 (2013).
- [13] J. L. Bohn, A. M. Rey, and J. Ye, Cold molecules: Progress in quantum engineering of chemistry and quantum matter, *Science* **357**, 1002 (2017).
- [14] N. Y. Yao, M. P. Zaletel, D. M. Stamper-Kurn, and A. Vishwanath, A quantum dipolar spin liquid, *Nat. Phys.* **14**, 405 (2018).
- [15] V. V. Albert, J. P. Covey, and J. Preskill, Robust Encoding of a Qubit in a Molecule, *Phys. Rev. X* **10**, 031050 (2020).
- [16] A. M. Kaufman and K.-K. Ni, Quantum science with optical tweezer arrays of ultracold atoms and molecules, *Nat. Phys.* **17**, 1324 (2021).
- [17] J. Ma, X. Wang, C. P. Sun, and F. Nori, Quantum spin squeezing, *Phys. Rep.* **509**, 89 (2011).
- [18] L. Pezzè, A. Smerzi, M. K. Oberthaler, R. Schmied, and P. Treutlein, Quantum metrology with nonclassical states of atomic ensembles, *Rev. Mod. Phys.* **90**, 035005 (2018).
- [19] T. Bilitewski, L. De Marco, J.-R. Li, K. Matsuda, W. G. Tobias, G. Valtolina, J. Ye, and A. M. Rey, Dynamical Generation of Spin Squeezing in Ultracold Dipolar Molecules, *Phys. Rev. Lett.* **126**, 113401 (2021).
- [20] H. J. Briegel and R. Raussendorf, Persistent Entanglement in Arrays of Interacting Particles, *Phys. Rev. Lett.* **86**, 910 (2001).

- [21] R. Raussendorf, D. E. Browne, and H. J. Briegel, Measurement-based quantum computation on cluster states, *Phys. Rev. A* **68**, 022312 (2003).
- [22] H. J. Briegel, D. E. Browne, W. Dür, R. Raussendorf, and M. Van den Nest, Measurement-based quantum computation, *Nat. Phys.* **5**, 19 (2009).
- [23] B. P. Lanyon, P. Jurcevic, M. Zwerger, C. Hempel, E. A. Martinez, W. Dür, H. J. Briegel, R. Blatt, and C. F. Roos, Measurement-Based Quantum Computation with Trapped Ions, *Phys. Rev. Lett.* **111**, 210501 (2013).
- [24] M. Mamaev, R. Blatt, J. Ye, and A. M. Rey, Cluster State Generation with Spin-Orbit Coupled Fermionic Atoms in Optical Lattices, *Phys. Rev. Lett.* **122**, 160402 (2019).
- [25] E. Kuznetsova, T. Bragdon, R. Côté, and S. F. Yelin, Cluster-state generation using van der Waals and dipole-dipole interactions in optical lattices, *Phys. Rev. A* **85**, 012328 (2012).
- [26] S. Ospelkaus, K.-K. Ni, G. Quémener, B. Neyenhuis, D. Wang, M. H. G. de Miranda, J. L. Bohn, J. Ye, and D. S. Jin, Controlling the Hyperfine State of Rovibronic Ground-State Polar Molecules, *Phys. Rev. Lett.* **104**, 030402 (2010).
- [27] J. A. Blackmore, P. D. Gregory, S. L. Bromley, and S. L. Cornish, Coherent manipulation of the internal state of ultracold $^{87}\text{Rb}^{133}\text{Cs}$ molecules with multiple microwave fields, *Phys. Chem. Chem. Phys.* **22**, 27529 (2020).
- [28] S. Kotochigova and D. DeMille, Electric-field-dependent dynamic polarizability and state-insensitive conditions for optical trapping of diatomic polar molecules, *Phys. Rev. A* **82**, 063421 (2010).
- [29] L. Caldwell, H. J. Williams, N. J. Fitch, J. Aldegunde, J. M. Hutson, B. E. Sauer, and M. R. Tarbutt, Long Rotational Coherence Times of Molecules in a Magnetic Trap, *Phys. Rev. Lett.* **124**, 063001 (2020).
- [30] S. Burchesky, L. Anderegg, Y. Bao, S. S. Yu, E. Chae, W. Ketterle, K.-K. Ni, and J. M. Doyle, Rotational Coherence Times of Polar Molecules in Optical Tweezers, *Phys. Rev. Lett.* **127**, 123202 (2021).
- [31] A. L. Collopy, M. T. Hummon, M. Yeo, B. Yan, and J. Ye, Prospects for a narrow line MOT in YO, *New J. Phys.* **17**, 055008 (2015).
- [32] A. L. Collopy, S. Ding, Y. Wu, I. A. Finneran, L. Anderegg, B. L. Augenbraun, J. M. Doyle, and J. Ye, 3D Magneto-Optical Trap of Yttrium Monoxide, *Phys. Rev. Lett.* **121**, 213201 (2018).
- [33] S. Ding, Y. Wu, I. A. Finneran, J. J. Bureau, and J. Ye, Sub-Doppler Cooling and Compressed Trapping of YO Molecules at μK Temperatures, *Phys. Rev. X* **10**, 021049 (2020).
- [34] Y. Wu, J. J. Bureau, K. Mehling, J. Ye, and S. Ding, High Phase-Space Density of Laser-Cooled Molecules in an Optical Lattice, *Phys. Rev. Lett.* **127**, 263201 (2021).
- [35] S. Truppe, H. J. Williams, M. Hambach, L. Caldwell, N. J. Fitch, E. A. Hinds, B. E. Sauer, and M. R. Tarbutt, Molecules cooled below the doppler limit, *Nat. Phys.* **13**, 1173 (2017).
- [36] L. Anderegg, B. L. Augenbraun, Y. Bao, S. Burchesky, L. W. Cheuk, W. Ketterle, and J. M. Doyle, Laser cooling of optically trapped molecules, *Nat. Phys.* **14**, 890 (2018).
- [37] J. F. Barry, D. J. McCarron, E. B. Norrgard, M. H. Steinecker, and D. DeMille, Magneto-optical trapping of a diatomic molecule, *Nature (London)* **512**, 286 (2014).
- [38] D. J. McCarron, M. H. Steinecker, Y. Zhu, and D. DeMille, Magnetic Trapping of an Ultracold Gas of Polar Molecules, *Phys. Rev. Lett.* **121**, 013202 (2018).
- [39] J. Aldegunde, B. A. Rivington, P. S. Żuchowski, and J. M. Hutson, Hyperfine energy levels of alkali-metal dimers: Ground-state polar molecules in electric and magnetic fields, *Phys. Rev. A* **78**, 033434 (2008).
- [40] M. L. Wall, K. R. A. Hazzard, and A. M. Rey, Quantum magnetism with ultracold molecules, in *From Atomic to Mesoscale*. (World Scientific, Singapore, 2015), p. 3.
- [41] See Supplemental Material at <http://link.aps.org/supplemental/10.1103/PhysRevLett.130.143002> for molecular Hamiltonians and interactions used in this work, the derivation of effective spin-spin interactions, and for an analysis of decoherence effects and experimental feasibility, which includes Refs. [42–63].
- [42] J. Aldegunde, H. Ran, and J. M. Hutson, Manipulating ultracold polar molecules with microwave radiation: The influence of hyperfine structure, *Phys. Rev. A* **80**, 043410 (2009).
- [43] J. Brown and A. Carrington, *Rotational Spectroscopy of Diatomic Molecules* (Cambridge University Press, Cambridge, England, 2003).
- [44] T. V. Tscherbul, J. Kłos, L. Rajchel, and R. V. Krems, Fine and hyperfine interactions in cold YbF-He collisions in electromagnetic fields, *Phys. Rev. A* **75**, 033416 (2007).
- [45] B. Neyenhuis, B. Yan, S. A. Moses, J. P. Covey, A. Chotia, A. Petrov, S. Kotochigova, J. Ye, and D. S. Jin, Anisotropic Polarizability of Ultracold Polar $^{40}\text{K}^{87}\text{Rb}$ Molecules, *Phys. Rev. Lett.* **109**, 230403 (2012).
- [46] W. G. Tobias, K. Matsuda, J.-R. Li, C. Miller, A. N. Carroll, T. Bilitewski, A. M. Rey, and J. Ye, Reactions between layer-resolved molecules mediated by dipolar spin exchange, *Science* **375**, 1299 (2022).
- [47] M. Foss-Feig, K. R. A. Hazzard, J. J. Bollinger, and A. M. Rey, Nonequilibrium dynamics of arbitrary-range Ising models with decoherence: An exact analytic solution, *Phys. Rev. A* **87**, 042101 (2013).
- [48] M. Mamaev, J. H. Thywissen, and A. M. Rey, Quantum computation toolbox for decoherence-free qubits using multi-band alkali atoms, *Adv. Quantum Technol.* **3**, 1900132 (2020).
- [49] A. M. Rey, L. Jiang, M. Fleischhauer, E. Demler, and M. D. Lukin, Many-body protected entanglement generation in interacting spin systems, *Phys. Rev. A* **77**, 052305 (2008).
- [50] A. L. Gaunt, T. F. Schmidutz, I. Gotlibovych, R. P. Smith, and Z. Hadzibabic, Bose-Einstein Condensation of Atoms in a Uniform Potential, *Phys. Rev. Lett.* **110**, 200406 (2013).
- [51] B. Mukherjee, Z. Yan, P. B. Patel, Z. Hadzibabic, T. Yefsah, J. Struck, and M. W. Zwierlein, Homogeneous Atomic Fermi Gases, *Phys. Rev. Lett.* **118**, 123401 (2017).
- [52] R. Bause, A. Schindewolf, R. Tao, M. Duda, X.-Y. Chen, G. Quémener, T. Karman, A. Christianen, I. Bloch, and X.-Y. Luo, Collisions of ultracold molecules in bright and dark optical dipole traps, *Phys. Rev. Res.* **3**, 033013 (2021).
- [53] A. S. Sørensen and K. Mølmer, Entanglement and Extreme Spin Squeezing, *Phys. Rev. Lett.* **86**, 4431 (2001).

- [54] A. Chu, P. He, J. K. Thompson, and A. M. Rey, Quantum Enhanced Cavity QED Interferometer with Partially Delocalized Atoms in Lattices, *Phys. Rev. Lett.* **127**, 210401 (2021).
- [55] W. B. Cairncross, J. T. Zhang, L. R. B. Picard, Y. Yu, K. Wang, and K.-K. Ni, Assembly of a Rovibrational Ground State Molecule in an Optical Tweezer, *Phys. Rev. Lett.* **126**, 123402 (2021).
- [56] P. D. Gregory, J. Aldegunde, J. M. Hutson, and S. L. Cornish, Controlling the rotational and hyperfine state of ultracold $^{87}\text{Rb}^{133}\text{Cs}$ molecules, *Phys. Rev. A* **94**, 041403(R) (2016).
- [57] J. Lin, J. He, M. Jin, G. Chen, and D. Wang, Seconds-Scale Coherence on Nuclear Spin Transitions of Ultracold Polar Molecules in 3D Optical Lattices, *Phys. Rev. Lett.* **128**, 223201 (2022).
- [58] J.-R. Li, K. Matsuda, C. Miller, A. N. Carroll, W. G. Tobias, J. S. Higgins, and J. Ye, Tunable itinerant spin dynamics with polar molecules, *Nature (London)* **614**, 70 (2023).
- [59] Q. Guan, S. L. Cornish, and S. Kotochigova, Magic conditions for multiple rotational states of bialkali molecules in optical lattices, *Phys. Rev. A* **103**, 043311 (2021).
- [60] K. Asnaashari and R. V. Krems, Quantum annealing with pairs of $^2\Sigma$ molecules as qubits, *Phys. Rev. A* **106**, 022801 (2022).
- [61] L. Liu, C.-L. Yang, M.-S. Wang, X.-G. Ma, and Y.-G. Yi, Spectroscopic properties of the low-lying electronic states and laser cooling feasibility for the SrI molecule, *Chin. J. Phys.* **71**, 435 (2021).
- [62] J. O. Schröder, C. Nitsch, and W. E. Ernst, Polarization spectroscopy of SrI in a heat pipe: The $B^2\Sigma^+-X^2\Sigma^+$ (0,0) system, *J. Mol. Spectrosc.* **132**, 166 (1988).
- [63] L. Anderegg, S. Burchesky, Y. Bao, S. S. Yu, T. Karman, E. Chae, K.-K. Ni, W. Ketterle, and J. M. Doyle, Observation of microwave shielding of ultracold molecules, *Science* **373**, 779 (2021).
- [64] F. Herrera, Y. Cao, S. Kais, and K. B. Whaley, Infrared-dressed entanglement of cold open-shell polar molecules for universal matchgate quantum computing, *New J. Phys.* **16**, 075001 (2014).
- [65] J. W. Park, Z. Z. Yan, H. Loh, S. A. Will, and M. W. Zwierlein, Second-scale nuclear spin coherence time of ultracold $^{23}\text{Na}^{40}\text{K}$ molecules, *Science* **357**, 372 (2017).
- [66] J.-Y. Zhang, Z.-W. Zhou, and G.-C. Guo, Eliminating next-nearest-neighbor interactions in the preparation of cluster state, *Chin. Phys. Lett.* **28**, 050301 (2011).
- [67] P. D. Gregory, J. A. Blackmore, S. L. Bromley, J. M. Hutson, and S. L. Cornish, Robust storage qubits in ultracold polar molecules, *Nat. Phys.* **17**, 1149 (2021).
- [68] B. Friedrich and D. Herschbach, Steric proficiency of polar $^2\Sigma$ molecules in congruent electric and magnetic fields, *Phys. Chem. Chem. Phys.* **2**, 419 (2000).
- [69] T. V. Tscherbul and R. V. Krems, Controlling Electronic Spin Relaxation of Cold Molecules with Electric Fields, *Phys. Rev. Lett.* **97**, 083201 (2006).
- [70] E. Abrahamsson, T. V. Tscherbul, and R. V. Krems, Inelastic collisions of cold polar molecules in nonparallel electric and magnetic fields, *J. Chem. Phys.* **127**, 044302 (2007).
- [71] M. A. Perlin, C. Qu, and A. M. Rey, Spin Squeezing with Short-Range Spin-Exchange Interactions, *Phys. Rev. Lett.* **125**, 223401 (2020).
- [72] E. Altuntaş, J. Ammon, S. B. Cahn, and D. DeMille, Demonstration of a Sensitive Method to Measure Nuclear-Spin-Dependent Parity Violation, *Phys. Rev. Lett.* **120**, 142501 (2018).
- [73] T. V. Tscherbul, J. Ye, and A. M. Rey, State-insensitive trapping conditions for microwave-dressed rotational states of polar molecules (to be published).